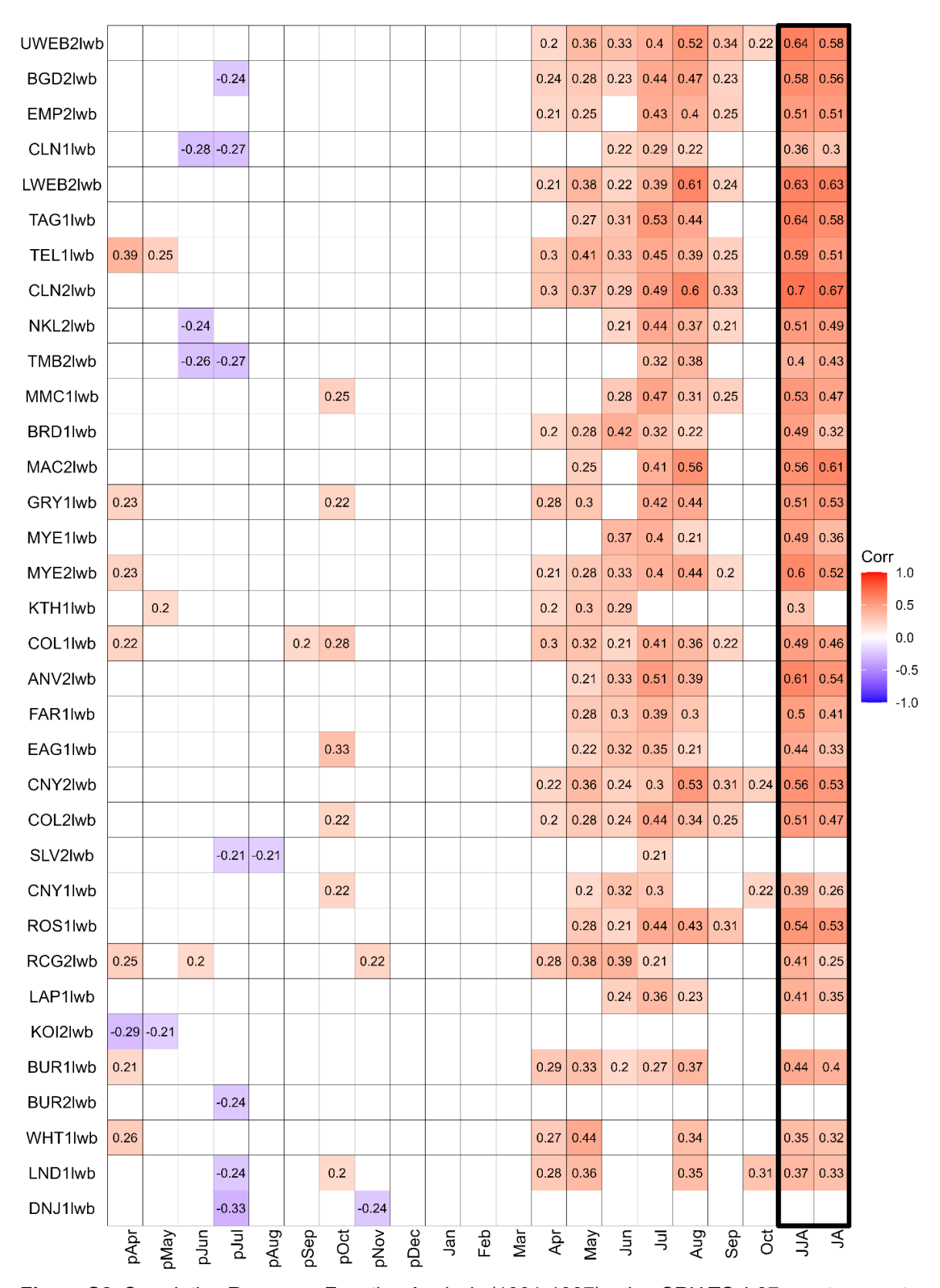
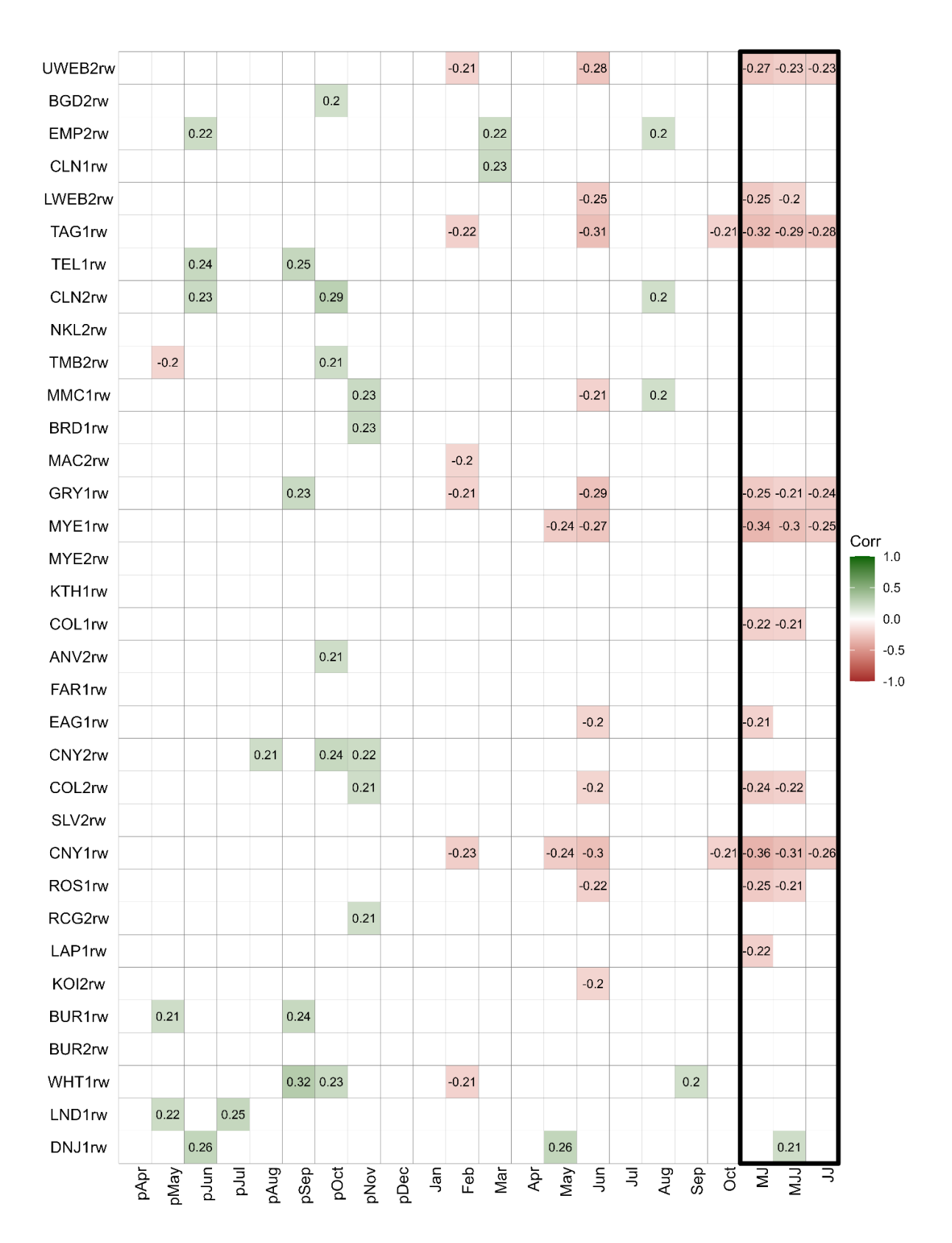


**Figure S1.** Correlation Response Function Analysis (1901-1997) using CRU TS 4.07 max temperatures with RW chronologies. Includes previous growing season, current growing season, and seasonal correlations. Sites are ordered by distance from upper treeline.



**Figure S2.** Correlation Response Function Analysis (1901-1997) using CRU TS 4.07 max temperatures with LWBI chronologies. Includes previous growing season, current growing season, and seasonal correlations. Sites are ordered by distance from upper treeline.



**Figure S3.** Correlation Response Function Analysis (1901-1997) using CRU TS 4.07 precipitation with RW chronologies. Includes previous growing season, current growing season, and seasonal correlations. Sites are ordered by distance from upper treeline.

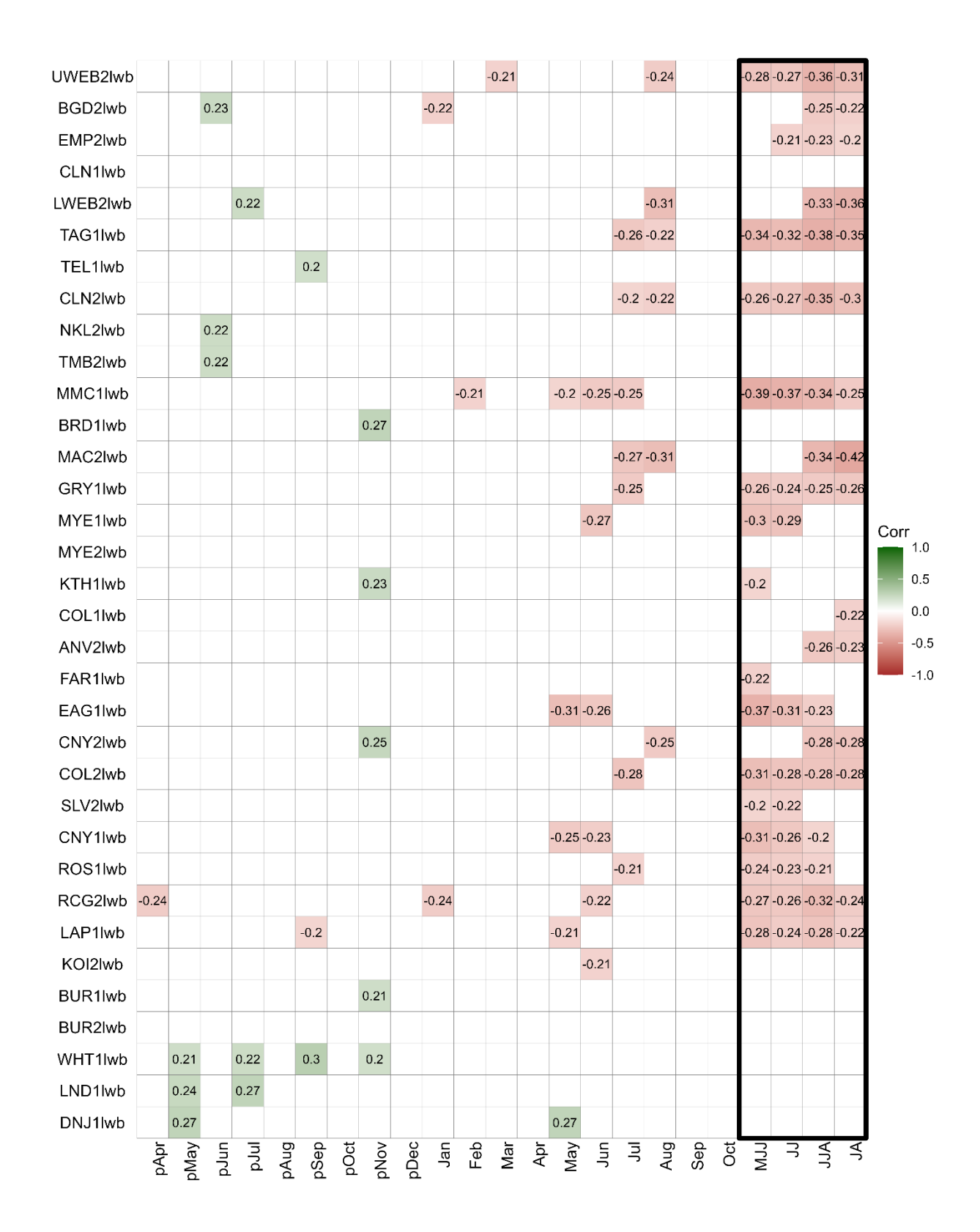


**Figure S4.** Correlation Response Function Analysis (1901-1997) using CRU TS 4.07 precipitation with LWBI chronologies. Includes previous growing season, current growing season, and seasonal correlations. Sites are ordered by distance from upper treeline.

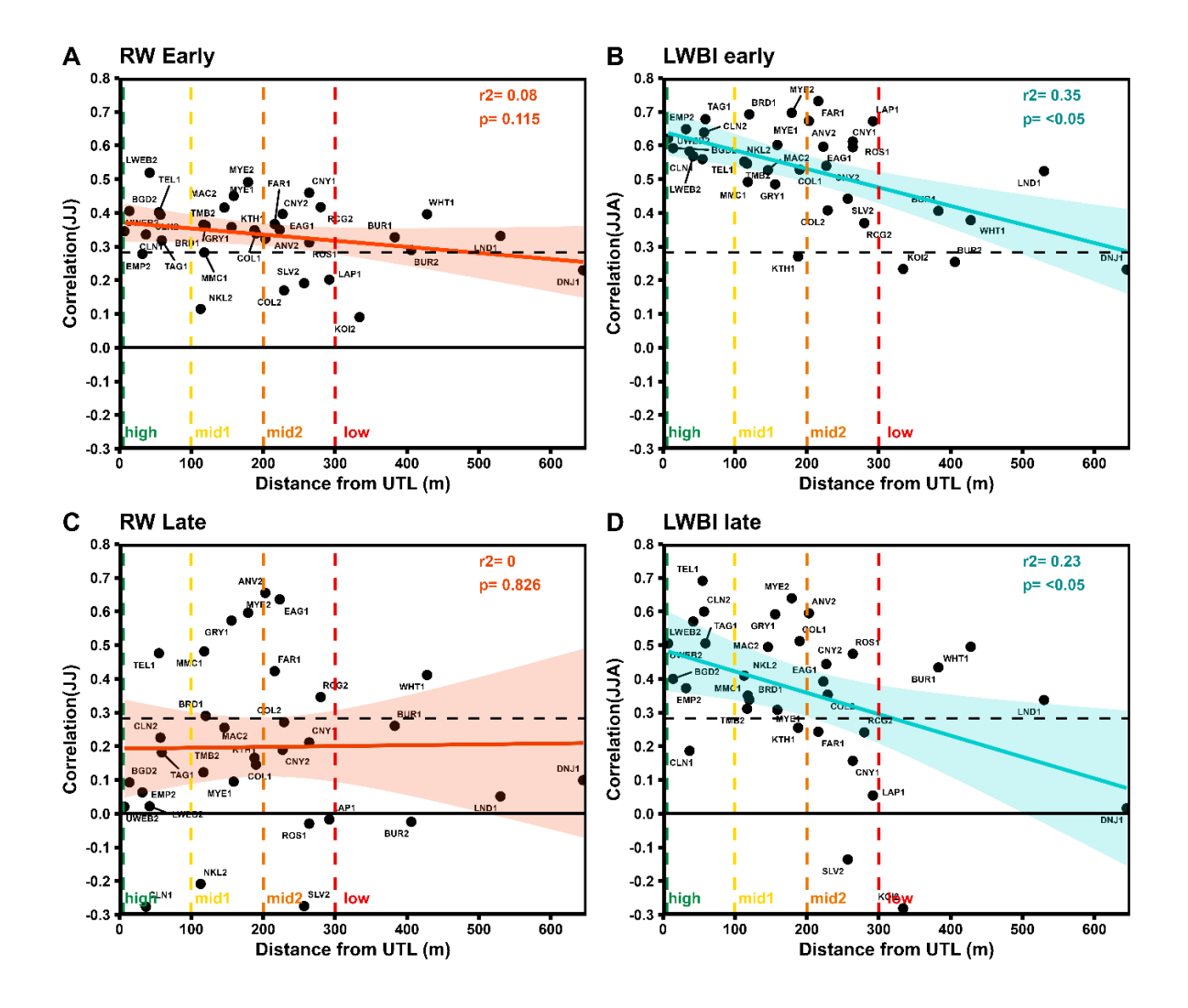


**Figure S5.** Split period relationship between dominant season correlation and distance from upper treeline (UTL) using **BEST** maximum temperature data (see Figure 2.3 for CRU TS 4.07 equivalent). **A.** Early period (1901-1944) June-July (JJ) RW correlations vs distance from UTL. **B.** Early period (1901-1944) June-July-August (JJA) LWBI correlations vs distance from UTL. **C.** Late period (1945-1997) JJ RW correlations vs distance from UTL. **D.** Late period (1945-1997) JJ LWBI. correlations vs distance from UTL. Linear functions added to each relationship. Coloured vertical lines denote boundaries for splitting chronologies into subgroups based on strength of the relationship.

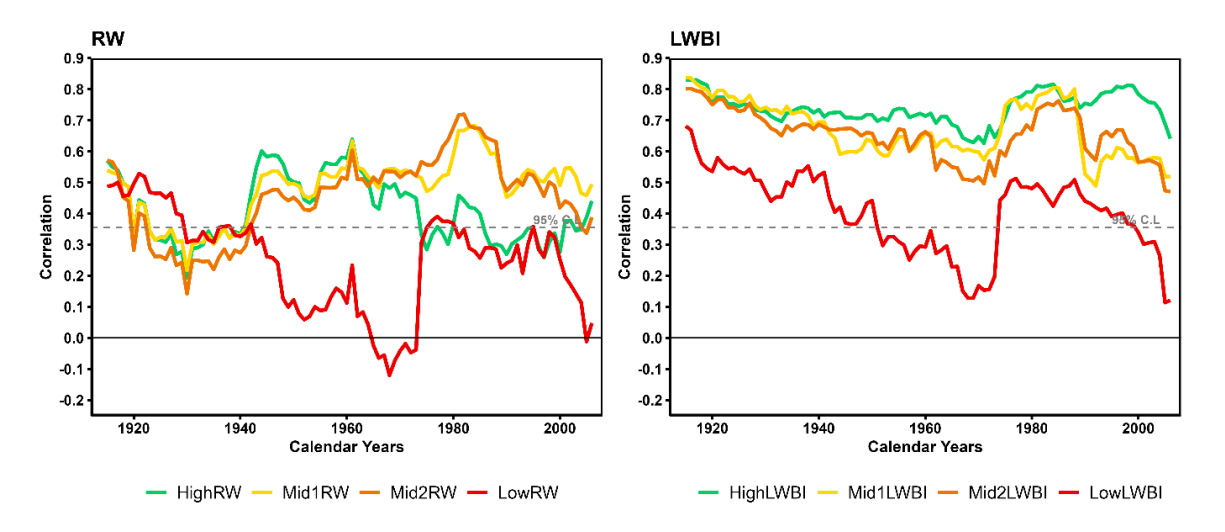


**Figure S6.** Running 31 years running Pearson's correlations between subgrouped chronologies and dominant season **BEST** Tmax. Dashed grey line denotes 95% confidence level.

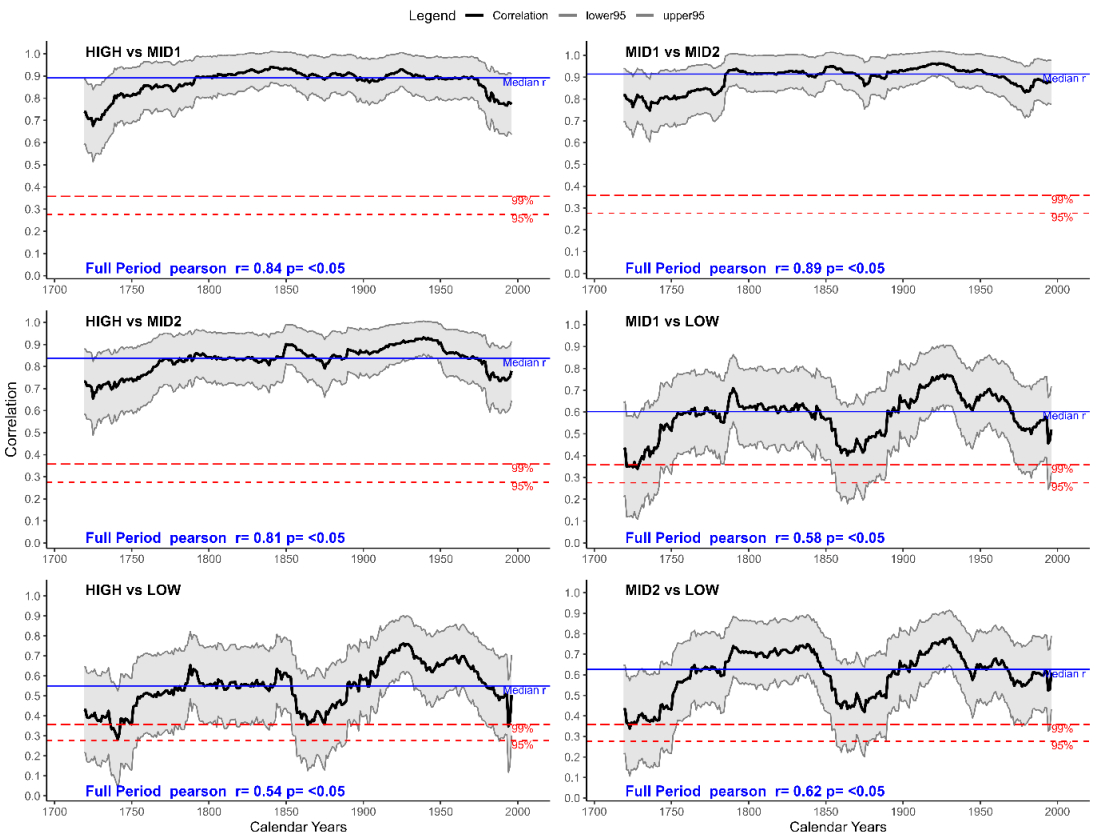


**Figure S7.** Between series Pearson correlations. 99% and 95% confidence levels denoted in red. Highlights a breakdown in the common signal between all other subgroups and the Low subgroup which contains sites furthest from upper treeline.

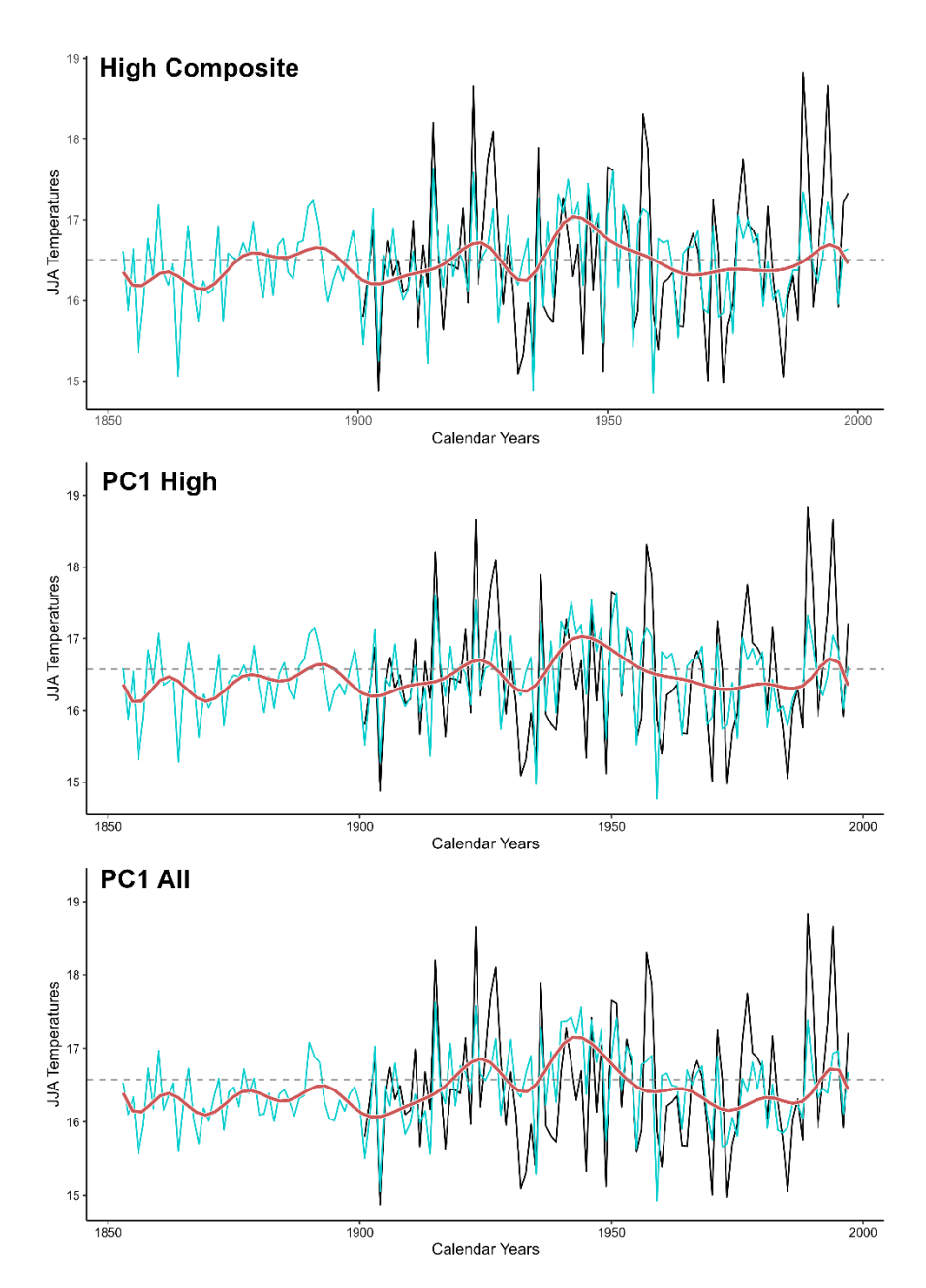


**Figure S8.** Comparison of the JJA reconstruction variants over the full common period (1853-1997). Calibration/Validation statistics are found in Table 2 in the main manuscript. Red line is a 20yr flexible spline added to assess the low frequency trends.

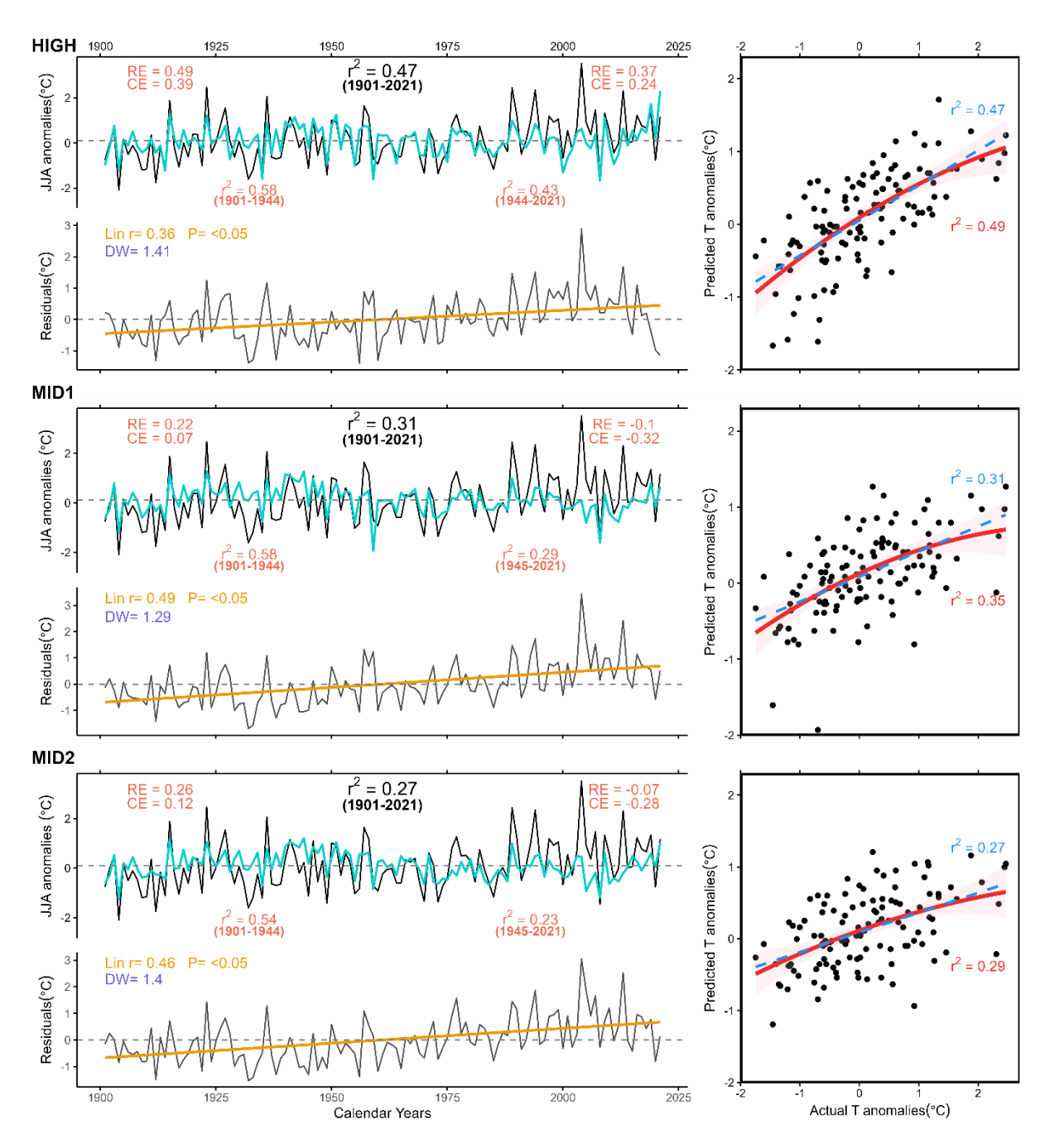


**Figure S9. BEST** Tmax full period reconstruction (1901-2021), residuals analyses, and actual vs predicted temperature anomalies. Full period  $r^2$ , calibration period  $r^2$  (1901-1944) and validation period  $r^2$  (1945-2021) represented in the upper plot of the left panels. Linear  $r^2$  of the residuals shown in yellow and Durbin Watson test for residual autocorrelation in purple. Scatter plots have a quadratic function plotted with error in red and the linear function in blue dashed line.

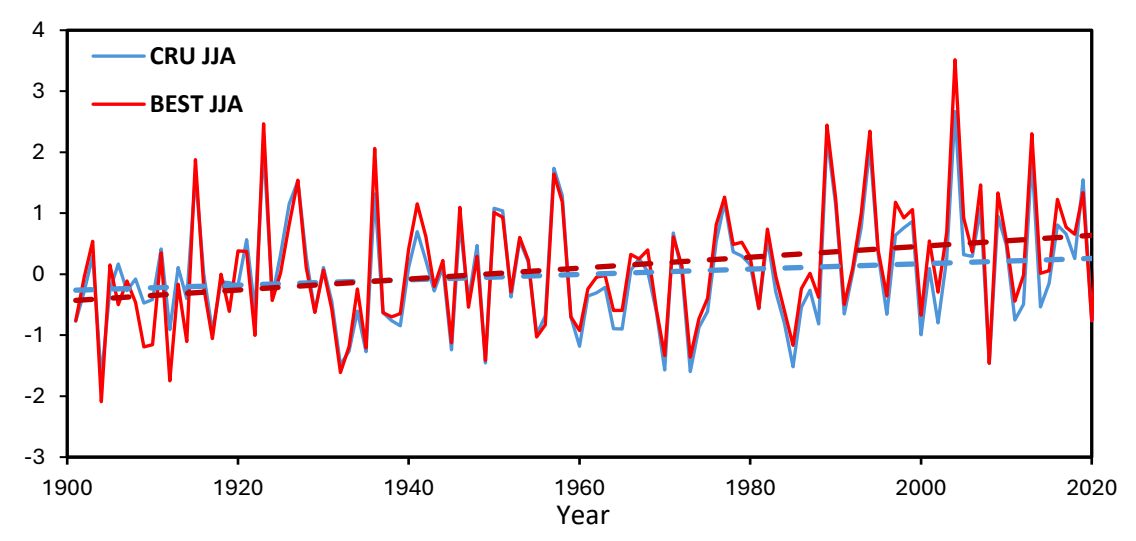
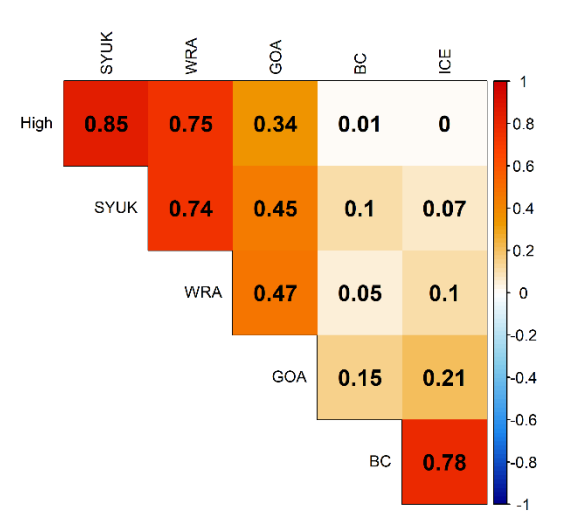


Figure \$10. Comparison of CRU TS JJA and BEST JJA Tmax.



**Figure S11.** Correlation matrix comparing optimum High LWBI chronology from this study with other existing NWNA chronologies.